J. Fluid Mech. (2011), *vol.* 673, *pp.* 245–254. © Cambridge University Press 2011
doi:10.1017/S002211201100053X

Geometry of valley growth

A. P. PETROFF[1]†, O. DEVAUCHELLE[1], D. M. ABRAMS[1]‡, A. E. LOBKOVSKY[1], A. KUDROLLI[2] AND D. H. ROTHMAN[1]

[1]Department of Earth, Atmospheric, and Planetary Sciences, Massachusetts Institute of Technology, Cambridge, MA 02139, USA

[2]Department of Physics, Clark University, Worcester, MA 01610, USA

(Received 8 November 2010; revised 8 November 2010; accepted 29 January 2011; first published online 14 March 2011)

Although amphitheatre-shaped valley heads can be cut by groundwater flows emerging from springs, recent geological evidence suggests that other processes may also produce similar features, thus confounding the interpretations of such valley heads on Earth and Mars. To better understand the origin of this topographic form, we combine field observations, laboratory experiments, analysis of a high-resolution topographic map and mathematical theory to quantitatively characterize a class of physical phenomena that produce amphitheatre-shaped heads. The resulting geometric growth equation accurately predicts the shape of decimetre-wide channels in laboratory experiments, 100 m-wide valleys in Florida and Idaho, and kilometre-wide valleys on Mars. We find that, whenever the processes shaping a landscape favour the growth of sharply protruding features, channels develop amphitheatre-shaped heads with an aspect ratio of π.

Key words: fingering instability, geophysical and geological flows, pattern formation

1. Introduction

When groundwater emerges from a spring with sufficient intensity to remove sediment, it carves a valley into the landscape (Dunne 1980). Over time, this 'seepage erosion' causes the spring to migrate, resulting in an advancing valley head with a characteristic rounded form (Lamb *et al.* 2006). Proposed examples of such 'seepage channels' include centimetre-scale rills on beaches and levees (Higgins 1982; Schorghofer *et al.* 2004), 100 m-scale valleys on Earth (Russell 1902; Wentworth 1928; Laity & Malin 1985; Orange, Anderson & Breen 1994; Schumm *et al.* 1995; Abrams *et al.* 2009) and kilometre-scale valleys on Mars (Sharp & Malin 1975; Higgins 1982; Malin & Carr 1999). Although it has long been thought that the presence of an amphitheatre-shaped head is diagnostic of seepage erosion (Higgins 1982; Laity & Malin 1985; Russell 1902), recent work suggests that overland flow can produce similar features (Lamb *et al.* 2006, 2008). To address this ambiguity, we seek a general characterization of processes that produce channels indistinguishable in shape from seepage channels.

We first identify the the interface dynamics (Ben-Jacob *et al.* 1983; Brower *et al.* 1983; Shraiman & Bensimon 1984; Kessler, Koplik & Levine 1985; Pelcé 1988,

† Email address for correspondence: petroffa@mit.edu

‡ Present address: Department of Engineering Sciences and Applied Mathematics, Northwestern University, Evanston, IL 60208, USA.

https://doi.org/10.1017/S002211201100053X Published online by Cambridge University Press

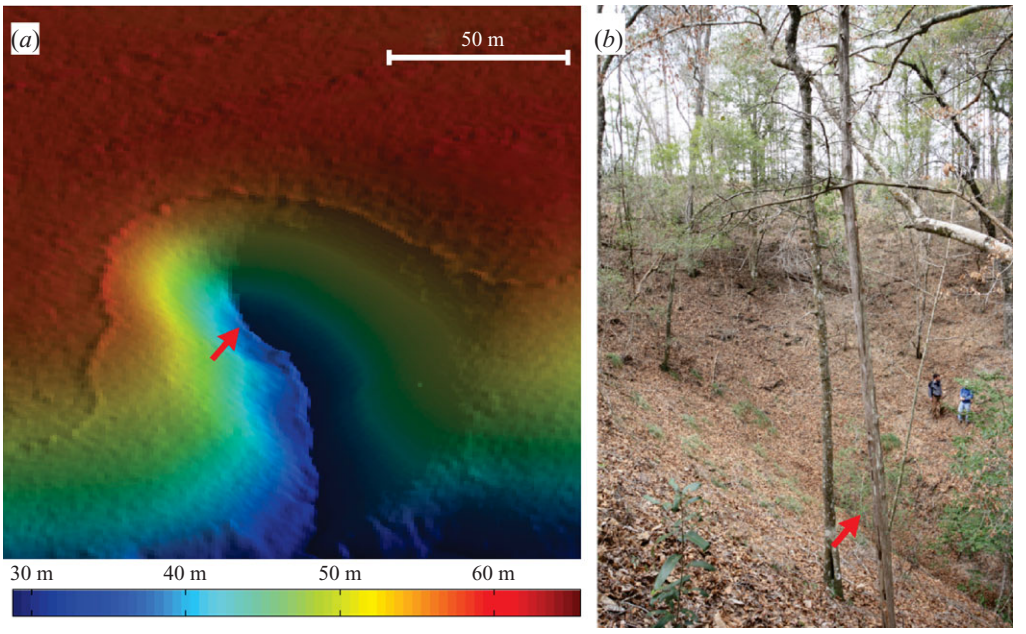


FIGURE 1. Examples of seepage valleys from the Florida network. (*a*) Topography obtained from a high-resolution map (Abrams *et al.* 2009) showing the rounded 'amphitheatre-shaped' valley head surrounding a spring (red arrow). Colours represent elevation above sea level. (*b*) A seepage valley head as viewed from the sidewall. The red arrow shows the approximate position of the spring. Note people for scale.

2004; Marsili *et al.* 1996) appropriate for amphitheatre-shaped valley heads formed by seepage erosion. We then show that the same dynamics apply in a more general setting. We find that whenever the processes shaping a landscape cause valleys to grow at a rate proportional to their curvature, they develop amphitheatre-shaped heads with a precise shape. This result clarifies the controversy surrounding terrestrial and Martian valleys by showing that many of these features are quantitatively consistent with a class of dynamics which includes, but is not limited to, seepage erosion.

2. The Florida network

To provide a precise context for our analysis, we first focus on a well-characterized kilometre-scale network of seepage valleys on the Florida Panhandle (Schumm *et al.* 1995; Abrams *et al.* 2009) (figure 1). This network is cut approximately 30 m into homogeneous, unconsolidated sand (Schumm *et al.* 1995; Abrams *et al.* 2009). Because the mean rainfall rate P is small compared to the hydraulic conductivity of the sand, nearly all water enters the channel through the subsurface (Schumm *et al.* 1995; Abrams *et al.* 2009). Furthermore, sand grains can be seen moving in streams near the heads, implying that the water drained by a spring is sufficient to remove sediment from the head. Finally, a myriad of amphitheatre-shaped valley heads ($n > 100$) allows for predictions to be tested in many different conditions.

We begin by finding the equilibrium shape of the water table in the Florida valley network. This shape describes how water is distributed between different heads. When the groundwater flux has a small vertical component (relative to the horizontal components), the Dupuit approximation (Bear 1979) of hydrology relates

https://doi.org/10.1017/S002211201100053X Published online by Cambridge University Press

the variations in the height h of the water table above an impermeable layer (Schumm *et al.* 1995; Abrams *et al.* 2009) to the mean rainfall rate P and the hydraulic conductivity K through the Poisson equation

$$\frac{K}{2}\nabla^2 h^2 + P = 0. \tag{2.1}$$

To simplify our analysis, we define two rescaled quantities: the Poisson elevation $\phi = (K/2P)^{1/2}h$ and the Poisson flux $q_p = \|\nabla\phi^2\|$. The Poisson elevation is determined entirely from the shape of the network and, consequently, can be measured from a map without knowledge of P or K. Physically, q_p is the area that is drained by a small piece of the network per unit arclength. It is, therefore, a local version of the inverse drainage density (i.e. the basin area divided by total channel length). By construction, the groundwater flux $q = Pq_p$. This measure of the flux differs from the geometric drainage area (Abrams *et al.* 2009) in that it is found from a solution of the Poisson equation, rather than approximated as the nearest contributing area.

Figure 2(*a*) shows the solution of (2.1) around the valley network (see supplementary material available at journals.cambridge.org/flm). Because the variations in the elevation at which the water table emerges are small (∼10 m) relative to the scale of the network (∼1000 m), we approximate the network boundary with an elevation contour extracted from a high-resolution topographic map (Abrams *et al.* 2009) on which ϕ is constant (see supplementary material). For a specified precipitation rate, this result predicts the flux q of water into each piece of the network.

To test this model of water flow, we compared the solution of (2.1) to measurements at 82 points in the network. Given a reported mean rainfall rate of $P = 5 \times 10^{-8}\,\mathrm{m\,s^{-1}}$ (Abrams *et al.* 2009), we find good agreement between observation and theory (figure 2*b*), indicating that (2.1) accurately describes the competition for groundwater. Additionally, we find that the water table elevation h is consistent with a ground penetrating radar survey (Abrams *et al.* 2009) of the area (see supplementary material). To understand how the distribution of groundwater through the network produces channels with amphitheatre-shaped heads, we proceed to relate the flux of water into a valley head to the geometry of the head.

3. Relation of flux and geometry

For an arbitrary network, there is no simple relationship between the flux of water into part of the network and its local shape. As each tip competes with every other part of the network, one can only find the local flux by solving (2.1). However, as first identified by Dunne (1980), valleys cut by seepage grow when sections of the valley which protrude outwards (high positive curvature) draw large fluxes while indented sections (negative curvature) of the network are shielded by the network. Motivated by this insight, we seek the relationship between the flux into a piece of a valley network and its planform curvature. Figure 2(*c*) shows that this relationship is consistent with a hyperbolic dependence of the Poisson flux (and hence the water flux) on the curvature. Consequently, at tips, where the curvature is high, this relationship can be approximated by the asymptote. Thus,

$$q_p \simeq \Omega\kappa, \tag{3.1}$$

where Ω is a proportionality constant related to the area drained by a single head. Thus, we find a local relationship between the processes shaping a seepage valley, represented by the flux q_p, and the local geometry, represented by the curvature κ. We

https://doi.org/10.1017/S002211201100053X Published online by Cambridge University Press

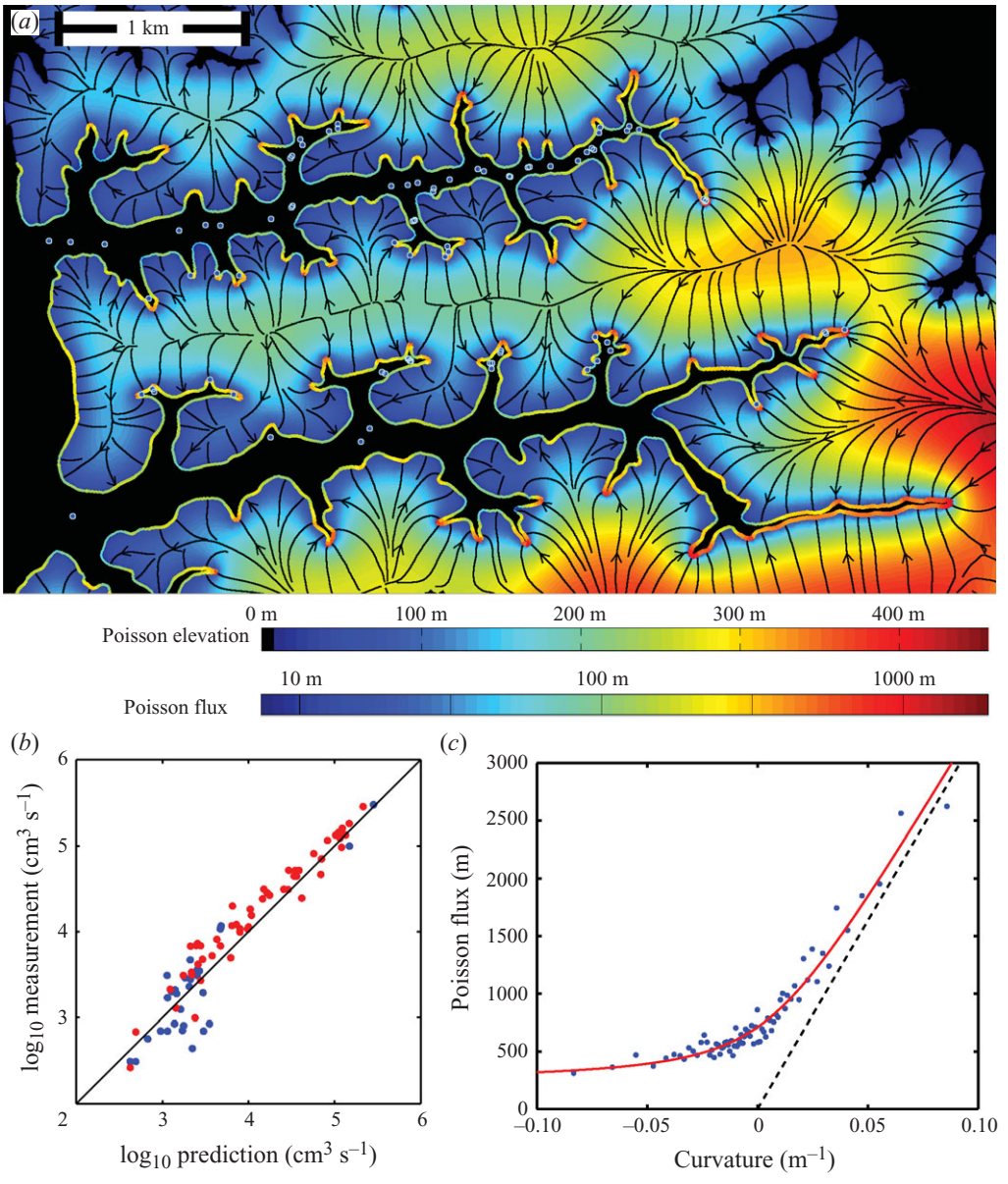


FIGURE 2. The water table and associated groundwater flux in the Florida network. (*a*) The magnitude of the Poisson flux (colour intensity on boundary) is the size of the area draining into a section of the network per unit length. It is found by solving (2.1) around the channels as approximated with an elevation contour. Flow lines are in black. The water discharge was measured at blue circles. The Poisson elevation and Poisson flux are proportional to the water table height and groundwater flux, respectively. (*b*) Comparison of the predicted discharge to measurements at 30 points in network taken in January 2009 (blue points) and 52 points in April 2009 (red points). The black line indicates equality. This comparison is direct and requires no adjustable parameters. (*c*) We observe a hyperbolic relationship between the curvature of the valley walls and the predicted flux (red curve). In regions of high curvature (i.e. valley heads) the flux is proportional to curvature (dashed line).

https://doi.org/10.1017/S002211201100053X Published online by Cambridge University Press

note that this relation may be further justified by a scaling argument (supplementary material), but here we merely employ it as an empirical observation.

4. Geometric growth law

In what follows we first ask how the flux–curvature relation (3.1) is manifested in the shape of a single valley head. To do so we first find the shape of a valley head that is consistent with the observed proportionality between groundwater flux and curvature. This derivation relies on three steps. First, (3.1) is converted, with an additional assumption, into a relationship between the rate at which a valley grows outward and its planform curvature. Next, we restrict our attention to valley heads that grow forward without changing shape. This condition imposes a geometric relationship between growth and orientation. Combining these, we find a relationship between curvature and orientation that uniquely specifies the shape of a valley growing forward due to groundwater flow. Finally, we find that our theoretical prediction is consistent both with valleys cut by seepage and systems in which seepage is doubtful. This result leads us to conclude that seepage valleys belong to a class of systems defined by a specific relationship between growth and curvature which includes seepage erosion as a particular case.

Following past work (Howard 1988; Abrams *et al.* 2009), we assume that the amount of sediment removed from the head is proportional to the flux of groundwater and, thus, by (3.1), $\Omega\kappa$. From (3.1), the speed c at which a valley grows outward is, therefore, proportional to the planform valley curvature κ. Setting H equal to the difference in elevation between the spring and the topography it is incising, the sediment flux is

$$Hc = \alpha\Omega\kappa, \tag{4.1}$$

where α is a proportionality constant with units of velocity. Equation (4.1) states that the more sharply a valley wall is curved into the drainage basin, the faster it will grow. The growth of the channel head is, therefore, 'curvature-driven' (Brower *et al.* 1983).

This derivation of (4.1) marks a shift of focus from the mechanics that shape a seepage valley to the dynamics by which it evolves. Although the specific processes of groundwater flow and sediment transport have not been addressed explicitly, this generalization has two advantages. First, (4.1) is purely geometric and can be solved to provide a quantitative prediction for the shape of a valley head. Equally importantly, the generality of these dynamics suggests that the class of processes they describe may extend beyond seepage valleys and thus provide a quantitative prediction for the evolution of a wider class of channelization phenomena.

5. Shape of a valley head

We restrict our attention to steady-state valley growth. When the channel grows forward at a speed c_0 without changing shape, the outward growth balances the growth forward. If θ is the angle between the normal vector and the direction the channel is growing (figure 3), then $c = c_0 \cos\theta$. Substituting this condition for translational growth into (4.1) relates the orientation of a point on the channel to the curvature at that point:

$$\cos\theta = \frac{\alpha\Omega}{c_0 H}\kappa(\theta), \tag{5.1}$$

https://doi.org/10.1017/S002211201100053X Published online by Cambridge University Press

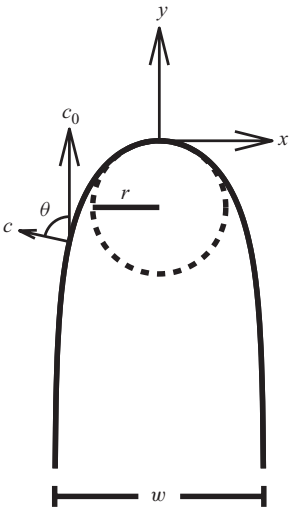


FIGURE 3. A balance between curvature-driven growth and translational growth sets the shape (5.2) of an amphitheatre-shaped valley head (solid black curve). When a curve evolves due to curvature-driven growth, the normal velocity c is inversely proportional to the radius of the best-fitting circle at that point. When a curve translates forward, there is a geometric relationship between the speed at which a point translates c_0 and the speed at which it grows in the normal direction c. This balance produces channels with a well-defined width w and an aspect ratio of $w/r = \pi$.

where $\kappa(\theta)$ denotes the dependence of curvature on orientation. Solving this equation (see the Appendix) for the shape of the curve with this property gives (Brower *et al.* 1983)

$$y(x) = \frac{w}{\pi} \log \cos\left(\pi \frac{x}{w}\right), \tag{5.2}$$

where $w = \pi\alpha\Omega/(c_0 H)$ is the valley width and $\theta = \pi x/w$. The planform shape $y(x)$ is shown in figure 3. A notable feature of this solution is that all geometric aspects of the channel head are set by the absolute scale of the valley (i.e. the valley width). In particular, it follows from (5.1) and (5.2) that all seepage channels have a characteristic aspect ratio

$$\frac{w}{r} = \pi, \tag{5.3}$$

where r is the radius of curvature of the tip (figure 3). By contrast, a semicircular valley head, in which $w = 2r$, has an aspect ratio of 2.

6. Comparison to observation

To test these predictions, we first compare the shape of elevation contours extracted from 17 isolated, growing tips in the Florida network to (5.2) and (5.3). As these valley heads vary in size, a sensible comparison of their shapes requires rescaling each channel to the same size; we, therefore, non-dimensionalize each curve by its typical radius $w/2$. To remove any ambiguity in the position where the width is measured, w is treated as a parameter and is fit from the shape of each valley head. Figure 4(a) compares all 17 rescaled channels heads to (5.2). Although each individual valley head may deviate from the idealization, the average shape of all valley heads fits the model well.

https://doi.org/10.1017/S002211201100053X Published online by Cambridge University Press

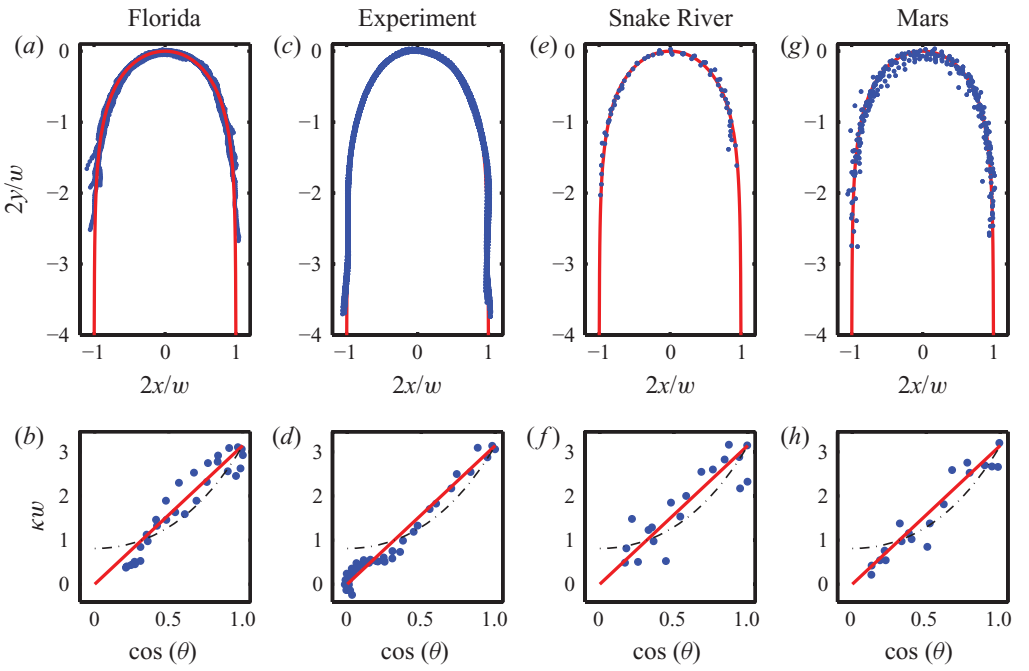


FIGURE 4. The shape of valley heads in the field, experiments, on Earth and on Mars are consistent with curvature-driven growth. (*a*) The shape of a channel produced by curvature-driven growth (red line) compared to the relative positions of points (blue dots) on the edge of valleys from the Florida network (17 elevation contours). (*b*) Comparison of the curvature at a point to the orientation (blue dots) of valleys from the Florida network. The red line is the linear relationship given in (6.1). The black dashed line corresponds to an ellipse with aspect ratio π. A semicircular head would predict the horizontal line $\kappa w = 2$. (*c–d*) The analogous plots for the experiments (25 elevation contours extracted at 3 min intervals). (*e–f*) The analogous plots for three valleys near Box Canyon and Malad Gorge. (*g–h*) The analogous plots for 10 Martian ravines.

This correspondence between theory and observation is further demonstrated by comparing the average curvature at a point to its orientation. We construct the average shape of the valley head by averaging the rescaled contours along the arclength. Rewriting (5.1) in terms of the width, we obtain

$$w\kappa = \pi \cos\theta. \tag{6.1}$$

Plotting $w\kappa$ as a function of $\cos\theta$, we indeed observe this proportionality (figure 4*b*). Moreover, the measured slope $p = 3.07 \pm 0.17$ is consistent with the predicted prefactor $p = \pi$. The proportionality relationship holds most clearly at high curvatures, where the approximation that flux scales with curvature is most accurate. Notably, were amphitheatre-shaped valley heads semicircular, then figure 4(*b*) would show the horizontal line $w\kappa(\theta) = 2$. If valley heads were sections of an ellipse with an aspect ratio of π, the data in figure 4(*b*) would follow the curve $w\kappa(\theta) = (4 + (\pi^2 - 4)\cos^2\theta)^{3/2}/\pi^2$. Viewing the semicircle and ellipse as geometric null hypotheses, we conclude from visual inspection of figure 4(*b*) that we can confidently reject them in favour of (5.2).

Seepage channels can also be grown in the laboratory by forcing water through a sand pile (Howard 1988; Schorghofer *et al.* 2004; Lobkovsky *et al.* 2007). Because these channels grow on the time scale of minutes to hours, one can directly

https://doi.org/10.1017/S002211201100053X Published online by Cambridge University Press

observe the development of the channels. Figure 4(*c*) compares (5.2) to elevation contours extracted from a previous experiment (Lobkovsky *et al.* 2007) while the channel is growing. Once the contours are rescaled and averaged, the curvature again is proportional to $\cos\theta$ (figure 4*d*). The measured proportionality constant $p = 3.07 \pm 0.13$, consistent with $p = \pi$.

7. Generalizations

The strong correspondence between (6.1) and the observed shapes of valley heads suggests that amphitheatre-shaped heads take their form from curvature-driven growth. Because curvature-driven growth is a simple geometric growth model, it likely characterizes a class of physical processes (Brower *et al.* 1983). For example, when a low-viscosity fluid is pushed slowly into a viscous fluid in two-dimensions, the diffusing pressure field deforms the intruding fluid into an elongated form as described by the Saffman–Taylor instability (Saffman & Taylor 1958). When stabilized by surface tension, the shape of the resulting 'viscous finger' is exactly that given in (5.2) (Bensimon *et al.* 1986; Combescot *et al.* 1986). This morphology has also been related to the shape of dendrites (Mullins & Sekerka 1963; Kessler, Koplik & Levine 1986) and is a steady-state solution to the deterministic Kardar–Parasi–Zhang equation (Kardar, Parisi & Zhang 1986).

This generality leads us to conjecture that when the growth of a valley head responds linearly to a diffusive flux, its dynamics at equilibrium reduce to curvature-driven growth. Geophysically relevant processes in which the growth may be dominated by a (possibly nonlinear) diffusive flux include the conduction of heat, topographic diffusion (Culling 1960), the shallow water equations (Chanson 1999) and elastic deformation (Landau & Lifshitz 1995). Thus, assuming appropriate boundary conditions exist, processes such as seasonal thawing, the relaxation of topography, overland flow and frost heave may produce valleys indistinguishable in planform shape from seepage channels.

To confirm the wide applicability of the geometric growth model, we proceed to compare (5.2) and (6.1) to enigmatic valleys on Earth and Mars. The origins of amphitheatre-shaped heads from the Snake River in Idaho (Russell 1902; Lamb *et al.* 2008) and the Martian valleys of Valles Marineris have been the subject of much debate (Sharp & Malin 1975; Higgins 1982; Malin & Carr 1999; Lamb *et al.* 2006). Figure 4(*e–h*) shows that the shape of valley heads in both of these systems is consistent with (5.2) and (6.1). Averaging the rescaled valleys and comparing the dimensionless curvature to the orientation, we find $p = 2.92 \pm 0.24$ and $p = 3.02 \pm 0.21$ for the Snake River and Martian features, respectively. Both estimates are consistent with $p = \pi$.

That these valleys are consistent with the predictions of curvature-driven growth does not necessarily imply that their growth was seepage-driven. We favour instead a more conservative conclusion: diffusive transport is ubiquitous and, therefore, so too is the $\log\cos\theta$ form.

8. Discussion

We have derived the shape of a valley head (5.2) from an observed relationship between the curvature of a valley head and the flux it receives (4.1). Two gaps remain in this derivation which make the appearance of valleys with the $\log\cos\theta$ form in natural settings somewhat mysterious. First, how does the intrinsically non-local process of

https://doi.org/10.1017/S002211201100053X Published online by Cambridge University Press

subsurface flow reduce to the purely local formulation of curvature-driven growth at the valley head? Additionally, how do sediment transport and subsurface flow stabilize the shape of the valley head once it reaches the $\log\cos\theta$ form? It is possible that the asymptotic proportionality between flux and curvature is a feature of Poisson fields under very general conditions. Similarly, sediment transport may contribute higher order corrections (Brower *et al.* 1983) to (4.1) which stabilize the growing valley head to small perturbations. Below we outline an alternative hypothesis.

An analogy to the classical Saffman–Taylor viscous finger (Saffman & Taylor 1958) offers some guidance. In steady state, a viscous finger translates forward at a constant speed and takes the form prescribed by (5.2); the normal velocity at each point is, therefore, proportional to the curvature. This relationship is, however, not intrinsic to viscous flows; it is instead a property of the dynamical steady state towards which the system evolves. It is possible that the appearance of the flux–curvature relation in geological settings represents a fixed point in the dynamics resulting from the coupling of topographic diffusion to subsurface flows. Somehow, despite the complexities of sediment transport and groundwater competition in a highly ramified network, the steady-state dynamics retain a simple geometric expression common to many phenomena.

This hypothesis may also explain why the shape of the valley head is stable even though (4.1) is not. Curvature-driven growth is an appropriate description of the dynamics shaping a valley head only when it is at equilibrium. To understand the stability of this shape, one must explicitly couple subsurface flows to the evolution of the topography.

9. Conclusion

Our results clarify the debate about the origin of amphitheatre-shaped valley heads by placing them within a class of dynamical phenomena characterized by growth proportional to curvature. From this qualitative distinction, we obtain a quantitative prediction: the valley head has a precisely defined shape with an aspect ratio of π. Regardless of the specific mechanical processes that cause a particular valley head to grow, all valley heads that fall within this dynamical class will look alike.

We would like to thank The Nature Conservancy for access to the Apalachicola Bluffs and Ravines Preserve, and K. Flournoy, B. Kreiter, S. Herrington and D. Printiss for guidance on the Preserve. We thank B. Smith for her experimental work. It is also our pleasure to thank M. Berhanu. This work was supported by Department of Energy Grant FG02-99ER15004. O.D. was additionally supported by the French Academy of Sciences.

Supplementary materials are available at journals.cambridge.org/flm.

REFERENCES

Abrams, D. M., Lobkovsky, A. E., Petroff, A. P., Straub, K. M., McElroy, B., Mohrig, D. C., Kudrolli, A. & Rothman, D. H. 2009 Growth laws for channel networks incised by groundwater flow. *Nature Geosci.* **28** (4), 193–196.

Bear, J. 1979 *Hydraulics of Groundwater*. McGraw-Hill.

Ben-Jacob, E., Goldenfeld, N., Langer, J. S. & Schön, G. 1983 Dynamics of interfacial pattern formation. *Phys. Rev. Lett.* **51** (21), 1930–1932.

Bensimon, D., Kadanoff, L. P., Liang, S., Shraiman, B. I. & Tang, C. 1986 Viscous flows in two dimensions. *Rev. Mod. Phys.* **58** (4), 977–999.

https://doi.org/10.1017/S002211201100053X Published online by Cambridge University Press

Brower, R. C., Kessler, D. A., Koplik, J. & Levine, H. 1983 Geometrical approach to moving-interface dynamics. *Phys. Rev. Lett.* **51** (13), 1111–1114.

Chanson, H. 1999 *The Hydraulics of Open Channel Flow: An Introduction*. Edward Arnold/ Butterworth-Heinemann.

Combescot, R., Dombre, T., Hakim, V., Pomeau, Y. & Pumir, A. 1986 Shape selection of Saffman-Taylor fingers. *Phys. Rev. Lett.* **56** (19), 2036–2039.

Culling, W. E. H. 1960 Analytic theory of erosion. *J. Geol.* **68**, 336–344.

Dunne, T. 1980 Formation and controls of channel networks. *Prog. Phys. Geogr.* **4** (2), 211–239.

Higgins, C. G. 1982 Drainage systems developed by sapping on Earth and Mars. *Geology* **10** (3), 147–152.

Howard, A. D. 1988 Groundwater sapping experiments and modeling. In *Sapping Features of the Colorado Plateau: A Comparative Planetary Geology Field Guide* (ed. A. D. Howard, R. C. Kochel & H. R. Holt), NASA SP-491, pp. 71–83.

Kardar, M., Parisi, G. & Zhang, Y. C. 1986 Dynamic scaling of growing interfaces. *Phys. Rev. Lett.* **56** (9), 889–892.

Kessler, D. A., Koplik, J. & Levine, H. 1985 Geometrical models of interface evolution. III. Theory of dendritic growth. *Phys. Rev.* A **31** (3), 1712–1717.

Kessler, D. A., Koplik, J. & Levine, H. 1986 Dendritic growth in a channel. *Phys. Rev.* A **34** (6), 4980–4987.

Laity, J. E. & Malin, M. C. 1985 Sapping processes and the development of theater-headed valley networks on the Colorado Plateau. *Geol. Soc. Am. Bull.* **96** (2), 203–217.

Lamb, M. P., Dietrich, W. E., Aciego, S. M., DePaolo, D. J. & Manga, M. 2008 Formation of Box Canyon, Idaho, by megaflood: implications for seepage erosion on Earth and Mars. *Science* **320** (5879), 1067–1070.

Lamb, M. P., Howard, A. D., Johnson, J., Whipple, K. X., Dietrich, W. E. & Perron, J. T. 2006 Can springs cut canyons into rock. *J. Geophys. Res.* E07002.

Landau, L. D. & Lifshitz, E. M. 1995 *Theory of Elasticity, Course of Theoretical Physics*, VII, 3rd revised edn., Vol. 7. Butterworth-Heinemann.

Lobkovsky, A. E., Smith, B. E., Kudrolli, A., Mohrig, D. C. & Rothman, D. H. 2007 Erosive dynamics of channels incised by subsurface water flow. *J. Geophys. Res.* F03S12.

Malin, M. C. & Carr, M. H. 1999 Groundwater formation of Martian valleys. *Nature* **397** (6720), 589–591.

Marsili, M., Maritan, A., Toigo, F. & Banavar, J. R. 1996 Stochastic growth equations and reparametrization invariance. *Rev. Mod. Phys.* **68** (4), 963–983.

Mullins, W. W. & Sekerka, R. F. 1963 Morphological stability of a particle growing by diffusion or heat flow. *J. Appl. Phys.* **34**, 323–329.

Orange, D. L., Anderson, R. S. & Breen, N. A. 1994 Regular canyon spacing in the submarine environment: the link between hydrology and geomorphology. *GSA Today* **4** (2), 35–39.

Pelcé, P. 1988 *Dynamics of Curved Fronts*. Academic.

Pelcé, P. 2004 *New Visions on Form and Growth: Fingered Growth, Dendrites, and Flames*. Oxford University Press.

Russell, I. C. 1902 Geology and water resources of the Snake River Plains of Idaho. *US Geol. Survey Bull.* **199**, 1–192.

Saffman, P. G. & Taylor, G. I. 1958 The penetration of a fluid into a porous medium or Hele-Shaw cell containing a more viscous liquid. *Proc. R. Soc. Lond. Ser. A, Math. Phys. Sci.* **245** (1242), 312–329.

Schorghofer, N., Jensen, B., Kudrolli, A. & Rothman, D. H. 2004 Spontaneous channelization in permeable ground: theory, experiment, and observation. *J. Fluid Mech.* **503**, 357–374.

Schumm, S. A., Boyd, K. F., Wolff, C. G. & Spitz, W. J. 1995 A ground-water sapping landscape in the Florida Panhandle. *Geomorphology* **12** (4), 281–297.

Sharp, R. P. & Malin, M. C. 1975 Channels on Mars. *Geol. Soc. Am. Bull.* **86** (5), 593–609.

Shraiman, B. & Bensimon, D. 1984 Singularities in nonlocal interface dynamics. *Phys. Rev.* A **30** (5), 2840–2842.

Wentworth, C. K. 1928 Principles of stream erosion in Hawaii. *J. Geol.* **36** (5), 385–410.

https://doi.org/10.1017/S002211201100053X Published online by Cambridge University Press